

# Optimal Continuum Synthesis of Partially Compliant Mechanisms for Prescribed Non-smooth Paths

Ashok Kumar Rai and Anupam Saxena  
Indian Institute of Technology, Kanpur, INDIA 208016  
Email: anupams@iitk.ac.in

## Abstract

In this paper, we synthesize partially compliant continua for prescribed non-smooth paths. In a novel contribution, optimal layout design of partially compliant mechanisms entails topology, shape and size synthesis with initially curved frame and rectilinear truss members of chosen materials. The analysis of partially compliant mechanisms having both pin joints as well as deformable members that can bend and/or stretch, is made possible through geometrically nonlinear finite element analysis in this work. Appearance of structural members in the base mesh is manipulated through discrete topology design variables that model member moduli. Element cross sections, end slopes of frame elements and nodal coordinates govern local shape and size. Deflection characteristics get enhanced not only by introducing the curvature in frame elements that influence both local bending and stretching, but also by the inclusion of truss elements that introduce only local stretching when needed. This along with the singularities introduced by the pin joints helps achieve a prescribed non-smooth path. We employ geometrically nonlinear finite element analysis using frame and truss elements to compare the design and prescribed paths using Fourier shape descriptors. As some variables are discrete, we employ a stochastic search through genetic algorithm. Numerical examples presented in this paper serve to illustrate the design intent.

## 1 Design Intent

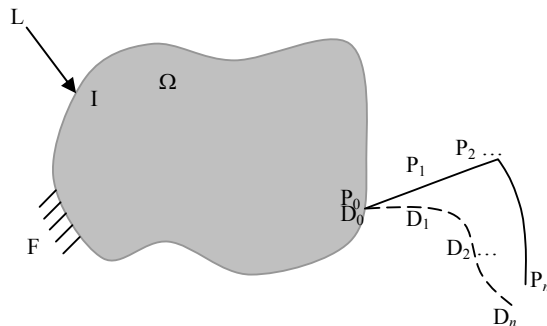


Fig. 1: Specifications for a partially compliant mechanism for non-smooth path generation.

The specifications to obtain an optimal partially compliant mechanism are shown in Fig. 1.  $\Omega$  is the region wherein optimal material connectivity is sought.  $F$  is the fixed boundary.  $L$  represents the input loads acting at prescribed input ports  $I$ .  $\{D_0, D_1, \dots, D_n\}$  is the output path obtained through a candidate design while  $\{P_0, P_1, \dots, P_n\}$  is the

prescribed path. The design intent is to determine the optimal layout comprising initially curved frame elements and truss elements along with their physical attributes (shape and size) and nature of connectivity (fixed or pinned) within the design region such that the discrepancy in shape, size and orientation between the design path and prescribed non-smooth path is minimized.

## 1.1 Related Work

Discrete elements were used previously to represent the design region in the topology synthesis of compliant mechanisms. Usually, element cross sections or their elastic moduli were employed as design variables. Frecker et al (1997)[1] employed full truss ground structure and used multi-criteria optimization to design small deformation compliant mechanisms. The ratio of the output deformation and strain energy was minimized. Synthesis was performed in two and a half dimensions with overlapping truss elements. As truss elements are not capable of capturing local bending, Saxena and Ananthasuresh (2000)[2] proposed to use a super ground structure of frame elements and designed optimal small deformation compliant topologies with generalized ratio based multi-criteria objectives. Lu and Kota (2003)[3] proposed a load path technique wherein the optimal topology generation was controlled through a set of paths of members sequentially juxtaposed and connecting the input, output and fixed nodes. Usually the output deformation is comparable to the overall size of the mechanism for which reason, large deformation models should be incorporated to capture deformations accurately. Saxena and Ananthasuresh (2001)[4] employed geometrically large deformation analysis and demonstrated the feasibility of obtaining optimal fully compliant mechanisms with prescribed nonlinear but smooth output paths. A least squared based metric that compared the prespecified and design paths was minimized. Sequential Quadratic Programming (SQP) was used to optimize the metric wherein the topology optimization problem was posed as a limiting case of size optimization. In previous works as well, mathematical programming schemes were used. Quite often, because of the presence of elements very near to their lower cross-sectional/elasticity bounds, convergence in analysis is not achieved due to which the search with the gradient based methods gets stalled and requires user intervention.

Saxena (2005a, b)[5] decoupled topology optimization from size optimization and achieved material assignment using discrete variables. Since gradient computation was not possible any longer, a genetic algorithm, which is a stochastic function-based optimization method, was used.

Size optimization was performed in addition using continuous variables, like cross sections and nodal coordinates. Output and specified paths were compared using the least squared metrics. Discrete material assignment strategy was generalized in Saxena (2005b)[6] who employed the barrier assignment approach to obtain optimal solutions with different prescribed materials. Parson and Canfield (2002)[7] earlier synthesized a family of small deformation compliant mechanisms using genetic algorithms by incorporating multiple objectives of maximizing the efficiency, geometric/mechanical advantage and compressive load. Zhou and Ting (2005)[8] used the spanning tree theory to synthesize compliant mechanisms using geometrically nonlinear analysis. Through this, they ensured material connectivity between the input and output ports and fixed nodes. They employed discrete cross sectional variables but retained the coupling between topology and size optimization. The cross section value of zero implied that the element was absent from the topology. Zhou and Ting (2006)[9] performed shape and size optimization using the wide curve theory. In both works, stochastic optimization was employed.

## 1.2 Motivation

The current research derives its motivation from three recent works on synthesis of compliant mechanisms mentioned below. Rai et al (2007)[10] demonstrated the significance of the use of initially curved frame elements in topology optimization. Initially curved frame elements exhibit a wider range of mechanical responses to applied loads. Mettlach (1996)[11] defined the characteristic deflection domain (CDD) for a compliant mechanism as an envelope of all possible points an output port can access in response to different applied loads. Mettlach (1996)[11] noted that the CDD of an initially curved beam of rectangular cross section and a variety of shapes, e.g., semicircular, S shapes etc was significantly larger. This is because the axial stiffness is much lower compared to an initially straight beam the tip of which traverses within a thin sliver. Rai et al (2007)[10] exploited this feature and established the feasibility of achieving prescribed curved paths with lesser number of members required to represent the design region.

Mankame and Ananthasuresh (2007)[12] synthesized compliant mechanisms for prescribed non-smooth paths using contact. They designed contact conditions around the optimal compliant continuum, while synthesizing the latter, such that the prescribed non-smooth path was traversed by the output port. A regularized contact model was used along with quasi-convexification techniques to facilitate the use of gradient based optimization. Mankame and Ananthasuresh (2007)[12] used Fourier Shape Descriptors (FSD) to formulate the objective. With these descriptors, the shapes of two simple, closed curves can be compared. Discrepancies between the overall lengths of the paths and their orientations were minimized as well. They argued that comparing the shape, size and orientation of the output paths independently was less restrictive than comparing the least squared discrepancy between the precision points of the design and prescribed paths. This is because the timing constraint wherein the output port needs to approach a

precision point at a certain time is eliminated. Mankame and Ananthasuresh (2007)[12] used initially straight frame elements to synthesize fully compliant mechanisms using the gradient based method. Both strategies have drawbacks. With initially straight frames, local deformation capabilities are not exploited as well as they are with initially curved frame elements. Further, gradient based methods can get stalled if at any stage, convergence in analysis is not achieved.

In addition to using conventional initially straight frame and truss elements, Ramrakhyani et al (2006)[13] employed especially formulated frames with one end fixed and other pinned to optimally locate pin joints in a partially compliant continuum. They demonstrated through a stochastic search via small deformation analysis that an optimal juxtaposition of an assortment of members (trusses, frames with one end fixed and those with both ends fixed) with varying local structural properties can be determined via topology optimization.

A non-smooth continuous curve is characterized by a function that is not differentiable at certain points. That is, the left and right slopes at a non-smooth point are not equal. With regard to the response, the output port changes its direction abruptly at a non-smooth point. There are several ways through which non-smoothness in the output response can be introduced. Mankame and Ananthasuresh (2007)[12] employed external contact to achieve a prescribed non-smooth output path. The notion is that an optimal compliant continuum comes in contact with an externally designed contact surface such that the trajectory of the output port gets altered abruptly. Instituting an external contact surface in the problem can be tedious and non-trivial – determination of the position, orientation, number and shapes of such contact surfaces can altogether be non-intuitive. The second way is to allow self contact between the constituting members of the mechanism to achieve a non-smooth path which has potential but has not been attempted as yet. The third way is to accomplish this through material nonlinearity, i.e., by allowing local plastic yielding of some members. This is undesirable since it will prevent cyclic use of the mechanism. The final approach is to optimally determine the type, shape and size of the members along with their interconnectivity such that a few desired intermediate ‘snap’ configurations, where continuum stiffness is singular or near singular, get introduced in the deformation profile of the compliant continuum and a prescribed non-smooth output path is obtained. Constituting members can stretch or compress (e.g., trusses), can additionally bend significantly (e.g., initially curved frames) or can be such that they can take only tensile loads (i.e., strings). Connectivity between members can either be fixed or pinned.

## 1.3 Layout of the paper

Novel contributions in this paper are summarized as follows. We synthesize the topology, shape and size of a partially compliant continuum of which the output port traverses a prescribed non-smooth path. We optimally determine the local deformation characteristics by using different member and joint types, that is, initially curved frame

elements and truss elements in the continuum. We employ discrete topology variables to choose between the member types and also to determine their state in the base mesh, i.e., whether they are present or absent. Shapes and sizes of all retained members are controlled using continuous variables. Thus, topology and parametric optimization are decoupled allowing for a more involved search. We first describe the initial domain layout and design variables used in the search in section 2. In section 3, we describe the geometrically nonlinear analysis using the two member types. This is entailed by the formulation of the objective in section 4 using the Fourier Shape Descriptors (FSD). The use of discrete variables in the formulation necessitates a stochastic search for which we have employed a genetic algorithm. Synthesis examples are presented in section 5, which is followed, by the discussion and conclusions in section 6.

## 2 Design Modeling

The base layout of the design is depicted in Fig. 2. Initial domain is rectangular in shape of size  $m \times n$  mm<sup>2</sup> where  $m$  and  $n$  are user-specified. The region is divided into a number of cells, each cell containing four members on the perimeter and four members in the interior. The members are shown with straight lines for ease in description. The members can either be present in or absent from the layout. If present, the members can either have bending and/or stretching/compression characteristics. That is, they can either emulate a truss or an initially curved frame element. Note that we do not include a fixed-pinned bending member due to manufacturing reasons. We surmise that it may not be straightforward to assemble such a member with the rest of the continuum. A truss member on the other hand can easily be pinned at both ends above the frame assemblage. Depending on the member characteristics, the junctions around and within each cell can either be fixed or pinned.

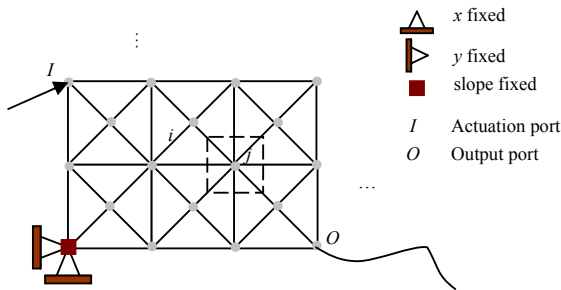


Fig. 2 Base mesh representing the design overall design specifications.

### 2.1 Topology Design and Member Choice Variables ( $v_i^T$ )

To each member  $i$  in the domain is assigned a variable  $v_i^T$  that can take the value of 0, 1 or 2.  $v_i^T = 0$  signifies that the member is absent from the basic layout.  $v_i^T = 1$  implies that the  $i^{\text{th}}$  member is an initially curved frame. The two end points of such a member are treated fixed. For

$v_i^T = 2$ , the  $i^{\text{th}}$  member is rendered the attributes of a truss element with the two end points pinned. Thus, with  $v_i^T$ , both local member and joint characteristics get determined. Note that the variable assignment for  $v_i^T$  is discrete, that is,  $v_i^T$  cannot take any value other than 0, 1 or 2. For  $v_i^T = 0$ , the shape and size variables in the genotype associated with the  $i^{\text{th}}$  member are not relevant. The shape and size design variables are discussed next.

### 2.2 Shape Design Variables ( $v_i^{s1}, v_i^{s2}$ )

Variables  $v_i^{s1}$  and  $v_i^{s2}$  are affiliated with only the initially curved frame elements. That is, these variables come into use only if the  $i^{\text{th}}$  member is designated as a frame element through  $v_i^T = 1$ . Variables  $v_i^{s1}$  and  $v_i^{s2}$  represent the two end slopes of the  $i^{\text{th}}$  member modeled as a Hermite cubic curve. These variables are continuous and vary between  $s_L$  and  $s_U$ , the user specified bounds for the end slopes.

### 2.3 Size Optimization Variables ( $v_i^w, v^{th}, v_j^x, v_j^y$ )

For both the initially curved frame or truss members, i.e., for  $v_i^T = 1$  or 2,  $v_i^w$  and  $v^{th}$  represent the in-plane width and out-of-plane thickness respectively. Variable  $v_i^w$  is local to the  $i^{\text{th}}$  member while  $v^{th}$  is a global variable. That is, the out-of-plane thickness of the entire continuum is controlled by a single variable. Both  $v_i^w$  and  $v^{th}$  are real valued varying between the user specified bounds  $[v_L^w, v_U^w]$  and  $[v_L^{th}, v_U^{th}]$  respectively. One can vary the out of plane thicknesses of each member which will make the search more comprehensive. However, this will result in  $N$  additional design variables in the genotype which will make the search process slow. Here,  $N$  is the number of members in the base mesh.

$[v_j^x, v_j^y]$  represent the coordinates of the  $j^{\text{th}}$  node in the base mesh. Following Hetrick and Kota (), nodal coordinates can be varied to govern the length of the truss members. The effective length of an initially curved frame also gets affected along with its shape through nodal perturbation. Variables  $v_j^x$  and  $v_j^y$  are continuous and are bounded within user specified values  $[v_L^x, v_U^x]$  and  $[v_L^y, v_U^y]$ .

### 2.4 Actuation Loads ( $F_k^x, F_k^y$ )

It was noted by Mankame and Ananthasuresh (2007) that fixing the magnitudes of the actuation loads a priori is not practical as their magnitudes cannot be judged accurately by the designer. Instead, actuation force magnitudes can be evolved along with the topology, shape and size variables. This provides additional design freedom. Let  $F_k^x$  and  $F_k^y$  be the force magnitudes along the horizontal and verti-

cal directions respectively – the directions of these forces and nodes on which they act are specified beforehand.  $F_k^x$  and  $F_k^y$  are used as continuous real design variables varying within the bounds  $[F_L^x, F_U^x]$  and  $[F_L^y, F_U^y]$ .

An array of all the aforementioned variables forms the genotype, a candidate design vector in the population of solutions in genetic algorithm used in this paper.

## 2.5 Other Design Parameters

Parameters that can have significant impact on the design are (i) the material properties, (ii) the boundary conditions and (iii) the input ports. They all can either be user specified or can be evolved as a part of the design. Within material properties are the elastic moduli of the members. If they are chosen to be evolved, there will be additional  $2N$  variables in the genotype. Further, at each node, we can specify at most 3 boundary conditions and that many number of actuation loads, though not simultaneously. Thus, we require a discrete variable to distinguish between free nodes in the base mesh, nodes that have some degrees of freedom or *dof* (horizontal, vertical and slope) fixed and the same that have some degrees of freedom actuated. Further, we will require three discrete variables per node to determine whether each of the three *dofs* is fixed/actuated or not. Finally, three other discrete variables will be required to assign the direction of actuation. This will additionally introduce a lot of variables in the genotype which will render the search very slow. In this work, we require the elastic properties, boundary and loading conditions to be the user specified parameters. The elastic moduli for frame and truss members, i.e.,  $E^F$  and  $E^T$  can be the same or different. Fixed and actuated *dofs* are also specified a priori along with the directions of the actuation loads. Their magnitudes, however, are evolved as a part of the design process.

## 2.6 Mesh Preprocessing for Design Evaluation

The genetic algorithm search implemented in this research works with a population of genotypes whose member design variables are depicted in Table 1. To evaluate the objective in section 3, each genotype is first converted into a phenotype. That is, the base mesh is preprocessed according to the information contained within the genotype. First, all members for which  $v_i^T = 0$  are removed from the base mesh. The resultant continuum may contain some disconnected elements or subregions. Elements belonging to all disconnected regions are identified and grouped. All dangling disconnected groups that do not contain the output port will not contribute to the output motion and, hence, are removed from the mesh. Retained members ( $v_i^T = 1$  or 2) and nodes are renumbered. Information that relates new and old node and element numbers is stored. To the initially curved frame elements retained, the corresponding end slopes, in-plane widths and out of plane thicknesses are transferred from the genotype. Likewise, the cross sec-

tional attributes are assigned to the retained truss members. Nodal coordinates are updated as per variables  $v_j^x$  and  $v_j^y$ .

To transfer the boundary and loading conditions, nodes on which such conditions are applied in the base mesh are checked for existence in the phenotype. If these nodes exist, the corresponding conditions are transferred along with the magnitudes of the actuation loads taken from the variables  $F_k^x$  and  $F_k^y$  in the genotype. Before analyzing the phenotype, the latter is preprocessed to check the following – (a) whether or not all actuation nodes are present, (b) if the output port is present and (c) if one or more nodes present in the phenotype are fixed. Phenotypes for which some input nodes are absent or the output port is absent are discarded at the outset. Only those that have all specified actuation and output *dofs* with a few *dofs* fixed are considered for analysis.

This preprocessing performed is an essential step before the analysis for two reasons – (i) the analysis is accurate with all input and output specifications ensured and (ii) the analysis is faster with the reduced number of structural members and degrees of freedom. Note that the members in the base mesh do not get removed permanently. These members can reappear through mutual interactions between the two candidate designs in the population using the crossover operator or through mutations on the topology design variables  $v_i^T$ .

## 3 Analysis of the Phenotype

We evaluate the performance of the phenotype using the geometrically nonlinear analysis briefed below. Deformation equations are formulated in the Total Lagrangian setting. Let  $\mathbf{F}(\mathbf{x}, \mathbf{u})$  and  $\mathbf{F}_e$  be the net internal and external force vectors where  $\mathbf{x}$  is the original configuration of the continuum with respect to the fixed reference frame and  $\mathbf{u}$  is the displacement vector measured in that frame. Let the force residual  $\mathbf{g}(\mathbf{x}, \mathbf{u})$  be defined as  $\mathbf{g}(\mathbf{x}, \mathbf{u}) = \mathbf{F}(\mathbf{x}, \mathbf{u}) - \mathbf{F}_e$ . We determine displacements such that  $\mathbf{g}(\mathbf{x}, \mathbf{u}) = \mathbf{0}$ . As the equilibrium equations are nonlinear, we achieve this iteratively. Using the Taylor series to expand  $\mathbf{g}(\mathbf{x}, \mathbf{u})$  about  $\mathbf{u}_i$  and setting it to  $\mathbf{0}$ , we get

$$\begin{aligned} \mathbf{g}(\mathbf{x}, \mathbf{u}_i + \Delta\mathbf{u}) &= \mathbf{g}(\mathbf{x}, \mathbf{u}_i) + \frac{\partial\mathbf{g}(\mathbf{x}, \mathbf{u}_i)}{\partial\mathbf{u}} \Delta\mathbf{u} = \mathbf{0} \\ \Rightarrow \Delta\mathbf{u} &= - \left[ \frac{\partial\mathbf{g}(\mathbf{x}, \mathbf{u}_i)}{\partial\mathbf{u}} \right]^{-1} \mathbf{g}(\mathbf{x}, \mathbf{u}_i) = -[\mathbf{K}_t(\mathbf{x}, \mathbf{u}_i)]^{-1} \mathbf{g}(\mathbf{x}, \mathbf{u}_i) \end{aligned} \quad (1)$$

Here,  $\mathbf{u}_i$  is the net displacement vector after the  $i^{\text{th}}$  iteration step,  $\Delta\mathbf{u}$  are the corrections in displacements and  $\mathbf{K}_t(\mathbf{x}, \mathbf{u}_i)$  is the *tangent stiffness matrix* evaluated at  $\mathbf{u}_i$ . The procedure delineated in Eq (1) is termed as the Newton-Raphson's iterative method. Note that  $\mathbf{K}_t(\mathbf{x}, \mathbf{u}_i) = \left[ \frac{\partial\mathbf{g}(\mathbf{x}, \mathbf{u}_i)}{\partial\mathbf{u}} \right] = \left[ \frac{\partial\mathbf{F}(\mathbf{x}, \mathbf{u}_i)}{\partial\mathbf{u}} \right]$  if the external forces  $\mathbf{F}_e$

do not depend on the displacements, e.g., in case of contact. Corrective displacements  $\Delta\mathbf{u}$  are computed in each iterative step and the net displacements are updated as  $\mathbf{u}_{i+1} = \mathbf{u}_i + \Delta\mathbf{u}$ . The iterations in Eq. (1) are performed until the

force residual is acceptably close to  $\mathbf{0}$ . In practice, we introduce the external forces in increments such that at the  $j^{\text{th}}$  increment,  $\mathbf{F}_e^j = \mathbf{F}_e^{j-1} + \Delta\mathbf{F}_e$ . After obtaining the equilibrium configuration for external forces at the  $(j-1)^{\text{th}}$  increment, we increment the external forces to  $\mathbf{F}_e^j$  and solve for the displacements using the Newton-Raphson's iterations. There are many texts, e.g., Crisfield (1991)[14] that document the nonlinear finite element analysis well. The internal force vector  $\mathbf{F}(\mathbf{x}, \mathbf{u})$  and the tangent stiffness matrix  $\mathbf{K}_t(\mathbf{x}, \mathbf{u})$  are assembled using the elemental internal force vectors  $\mathbf{f}^G(\mathbf{x}, \mathbf{u})$  and  $\mathbf{k}_t(\mathbf{x}, \mathbf{u})$ . Mankame (2004)[17] describes in detail the derivation of internal force vector and stiffness matrix for initially curved frame elements using the corotational formulation following (Crisfield 1991; Belytschko and Glaum 1979[15]; Belytschko and Hsieh 1973[16]). Crisfield (1991) describes the same for large deformation truss members. To be consistent with the enumeration of the *dofs* of frame elements, for truss elements, the global (forces/displacements) degrees of freedom are numbered such that at node  $i$ , the horizontal degree of freedom is represented by the  $(3i-2)^{\text{th}}$  entry while the vertical one is given by the  $(3i-1)^{\text{th}}$  one. The moment *dof* is represented using the  $(3i)^{\text{th}}$  entry. Accordingly,  $\mathbf{f}_i^G$  is expanded into a vector with 6 entries, the 3<sup>rd</sup> and the 6<sup>th</sup> entries corresponding to the internal moments. As the truss element does not take the moments at the pin joints, the corresponding moment entries in  $\mathbf{f}_i^G$  are taken as zero.

Thus, the extended  $\mathbf{f}_i^G$  appears as  $[f_1 \ f_2 \ 0 \ f_3 \ f_4 \ 0]^T$ . The element stiffness matrix is also expanded to have  $6 \times 6$  entries by letting the entries in the 3<sup>rd</sup> and 6<sup>th</sup> rows and columns to be zero. However, the diagonal entries corresponding to the moment degrees of freedom are arbitrarily chosen to be small values. This is equivalent to numerically introducing torsional springs of very small stiffnesses at the two ends of the truss member such that the global tangent stiffness matrix is near but not singular and inverting it is still possible as required by the Newton-Raphson iterations.

#### 4 Efficient Comparison of the output paths

Once the entire output path history is obtained for a candidate design through the analysis described above, we use the measure formulated in this section to compare how proximal the path is in shape, length and orientation to the prescribed non-smooth one. The least squared functions based on precision points used previously to compare the output paths are inadequate and restrictive. They are inadequate because they do not account for the path shape in between the precision points. Further, since it is required for the precision points to ideally coincide, restrictions creep in from the viewpoint that such correspondence is sought in certain time intervals. We employ Fourier shape descriptors to compare the output paths. These not only capture the path shapes but also comparison using these measures is independent of the temporal history. Following Ullah and Kota (1997)[18], Mankame and Ananthasuresh

(2007) and Rai et al (2007) have successfully employed these functions to compare output paths.

The shape of a planar curve can be characterized using a function that represents the change in angular direction of the curve as a function of the arc length. The function is periodic for a simple closed curve with a period corresponding to the length of the curve. If the normalized form of this periodic function is expanded using Fourier series, the coefficients of a truncated expansion are called Fourier shape descriptors. The coefficients of the low order terms in the expansion contain information about the overall shape of the curve.

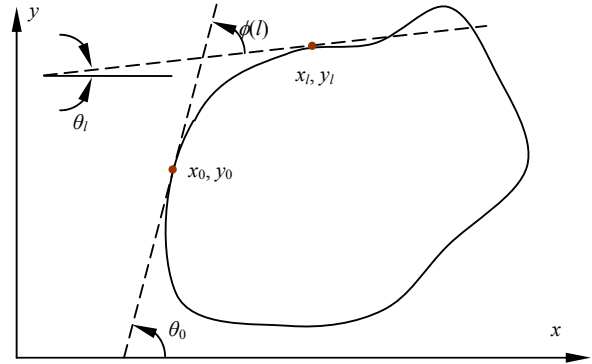


Figure 3 Cumulative Angular function for a closed, simple one

In cases like those in this paper where curves, whose shapes are to be compared are open, they can be closed by specifying a suitable start point such that the curves are not self intersecting. Consider a simple, closed curve described in a clockwise sense starting from the point  $(x_0, y_0)$  as shown in Fig. 3. The inclination of the tangent to the curve at this point is  $\theta_0$ . If the inclination of the tangent at the point  $(x_i, y_i)$  is  $\theta_i$ , the cumulative angular function is defined as

$$\phi(l) = \theta_i - \theta_0$$

If the total arc length of the curve is  $L$ ,  $\phi(L) = -2\pi$  for all smooth, simple, closed and clockwise oriented curves. However, at  $l = L$ ,  $\phi(l = 0) = 0$ . The following normalized form is used as a measure of shape which is invariant under rotations, translations and change in length.

$$\phi^*(t) = \phi\left(\frac{Lt}{2\pi}\right) + t$$

where  $t = 2\pi l/L$ ,  $t \in [0, 2\pi]$  is the normalized arc length. Note that  $\phi^*(0) = \phi^*(2\pi) = 0$ . As  $\phi^*(t)$  is a periodic function, it can be expanded into a Fourier series as

$$\phi^*(t) = a_0 + \sum_{k=1}^{\infty} (a_k \sin kt + b_k \cos kt) \quad (2)$$

Fourier shape descriptors are the coefficients  $a_k$  and  $b_k$ . For a path specified using discrete points, and that obtained in discrete points as a result of the analysis in section 3, let  $V_i$  denote the  $i^{\text{th}}$  vertex of a piece-wise linear, simple, closed, planar curve shown in Figure 4. The vertices are labeled clockwise as indicated in the figure starting from  $V_0$ . This can be chosen as a dummy point in case the two paths

compared are the open non-self intersecting paths. The change in the angular direction at  $V_i$  is indicated as  $\Delta\phi_i$  and the length of the segment between the vertices  $V_{(i-1)}$  and  $V_i$  is  $\Delta l_i$ . Noting that 1,  $\sin(kt)$  and  $\cos(kt)$  terms are orthogonal with respect to the inner product defined as  $\langle p, q \rangle = \int_0^{2\pi} p \cdot q dt$  where  $p$  and  $q$  are any 1,  $\sin(kt)$  and  $\cos(kt)$  with  $p \neq q$ , the Fourier coefficients can be found as follows

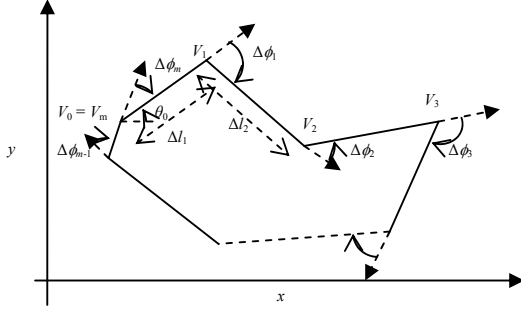


Figure 4 Details of linear piece-wise closed planar curve

$$a_0 = -\pi - \frac{1}{L} \int_0^L d\phi(l)l \approx -\pi - \frac{1}{L} \sum_{k=1}^N \Delta\phi_k l_k \quad (3)$$

noting that  $\phi(0) = 0$  and  $\phi(L) = -2\pi$ . Likewise

$$a_n = -\frac{1}{\pi n} \sum_{k=1}^N \Delta\phi_k \sin\left(\frac{2\pi n l_k}{L}\right) \quad (4)$$

and

$$b_n = -\frac{1}{\pi n} \sum_{k=1}^N \Delta\phi_k \cos\left(\frac{2\pi n l_k}{L}\right) \quad (5)$$

where  $l_k = \sum_{i=1}^k \Delta l_i$ ,  $A_n = \sqrt{a_n^2 + b_n^2}$  and  $\alpha_n = \arctan\left(\frac{a_n}{b_n}\right)$ .

Let for the user specified path the Fourier coefficients be  $\tilde{a}_k$  and  $\tilde{b}_k$  and for the response path, the coefficients be  $a_k$  and  $b_k$ . Let the length of user specified path be  $\tilde{L}$  and that of the response path be  $L$ . The initial path orientation angles are  $\tilde{\theta}_0$  and  $\theta_0$  respectively. The error in shape coefficients and other parameters can be calculated as

$$\begin{aligned} a_{err} &= \sum_{k=1}^N (a_k - \tilde{a}_k)^2 \\ b_{err} &= \sum_{k=1}^N (b_k - \tilde{b}_k)^2 \\ L_{err} &= (L - \tilde{L})^2 \\ \theta_{err} &= (\theta_0 - \tilde{\theta}_0)^2 \end{aligned} \quad (6)$$

#### 4.1 The objective formulation and design accomplishment

Based on the errors in shape, lengths and orientations of the paths described above, we formulate the objective below.

$$\text{Minimize } \psi = C_a a_{err} + C_b b_{err} + C_L L_{err} + C_\theta \theta_{err} \quad (P1)$$

$$\text{over } \mathbf{v} = \left\{ \begin{array}{l} v_i^T | v_i^T \text{ is discrete} \\ v_i^{s1} \quad v_i^{s2} \quad v_i^w \quad v_i^h \quad v_j^x \quad v_j^y \quad F_k^x \quad F_k^y | \text{ all real, continuous} \end{array} \right\}$$

Subject to:

1.  $\mathbf{F}(\mathbf{x}, \mathbf{u}^{(i)}) = \mathbf{F}_{ext}^{(i)}$
2.  $v_i^T = 0, 1 \text{ or } 2$
3.  $\mathbf{v}_{LB} \leq \mathbf{v} \leq \mathbf{v}_{UB}$
4. no contact between frame elements
5. number of input and output ports as specified.

The first constraint refers to the overall equilibrium after each increment  $i$  of the external force vector  $\mathbf{F}_{ext}$  is applied. The second constraint implies that the topology design variable  $v_i^T$  can take only integer values as shown to control the member appearance and characteristics. The third constraint signifies that all other continuous variables in  $\mathbf{v}$  are bounded within the lower and upper bounds  $\mathbf{v}_{LB}$  and  $\mathbf{v}_{UB}$ .

In partially compliant mechanisms synthesized in this work, overlap between the truss and frame members and that between two truss members is allowed. This is to accommodate one or more revolute joints at a joint site in the continuum. However, frame members are assumed to be on the same plane and they are not allowed to interact during deformation as signified through constraint 4. We have not implemented contact modeling and interaction between two frame elements implies that they will intersect during deformation which is not physically viable in our model. We have avoided such an interaction through a procedure described in Rai et al (2007). The fifth constraint ensures that an optimal mechanism retains all input and output conditions as specified prior to its design.

We accomplish the optimal design of a partially compliant mechanism by minimizing the objective in (P1). As one component of the design variable is discrete in nature modeled to recognize truss or frame members and to control their presence/absence in the base mesh, we employ a function based genetic algorithm (GA) search. Note that the implementation of a stochastic search is a necessity since gradient computation is not possible when discrete design variables are used. Another advantage of using GA is its feature that gives the ability to evaluate a population of solutions in a given generation. The constraints posed in the objective are strict and many candidate designs fail to meet them. Only a few survive that are passed on to the next generation for further improvement. A con of course is the large number of function evaluations involved which is time wise costly. We have employed a conventional

genetic algorithm as a search procedure in our work which is detailed in Rai et al (2007).

## 5 Synthesis Examples

We present two examples to illustrate the synthesis of partially compliant mechanisms. In the first example, an L-shaped output path is sought, while in the second, the output port of the mechanism is expected to follow a prescribed Z-shaped contour.

### 5.1 Synthesis for a prescribed L-shaped path

The design domain is of size  $100 \times 100 \text{ mm}^2$  and is discretized using 60 candidate members with 25 nodes, as shown in Fig. 5 (a). The nodes labeled “E” are fixed to the ground. A horizontal input actuation is applied at the node “I” in the negative  $x$ -direction, while node “P” is the output port. The specified output path is shown in Fig. 5 (b). As we can employ the Fourier arbitrary points for closed paths, we specify an additional arbitrary point, P\* to convert the prescribed output path into a simple closed curve. P\* in this example is near  $(-6, -4)$ . The arc length for the desired path is about 37 mm, approximately 37% of the characteristic dimension (100 mm) of the design domain.

There is no external load resisting the motion of the output port. It is not straightforward to include a prescribed output resistance in the synthesis procedure, if the nature of the output resistance is not known throughout the deformation history. The output path will significantly depend on the output resistance and will arbitrarily vary with output resistances modeled differently. Hence, the output resistance is omitted for the examples in this work. The topology, shape, and size optimization variables make up 352 in number. The  $x$ - and  $y$ -coordinates of the nodes are varied within the range of 5 mm each. Optimal widths and thickness are varied between 2 mm and 6 mm. The slopes for the initially curved frame elements are varied between  $-0.4$  and  $0.4$  radians. The lower and upper limits for the input force are taken as 30 N and 30 N, respectively. That is, the magnitude of the input load is not optimized as a design variable. For the initially curved frame elements, the elastic modulus is chosen as  $2000 \text{ Nmm}^{-2}$  while for the truss elements, it is taken as  $1000 \text{ Nmm}^{-2}$ . Coefficients used for terms in the objective are 10.0, 10.0, 1.0, and 1.0 for  $a_{\text{err}}$ ,  $b_{\text{err}}$ ,  $L_{\text{err}}$ , and  $\alpha_{\text{err}}$ , respectively. The population size for this example is 40. The number of generations for which optimization is performed is 3000. Crossover and mutation probabilities are 0.95 and 0.05, respectively. Six elite solution vectors from the old population replace the same number of worst ones in the new population.

The optimal mechanism is shown in Fig. 5 (c) in its undeformed configuration. Members shown in grey (red) are the initially curved frame members and those shown using dark (black) are the truss elements. The optimal partially compliant mechanism at different stages of actuation and tracing the response path is shown through Figures 5 (d) - (f). Figure 5 (b) also shows the magnified comparison between the response and specified paths. The specified path

is shown using ‘\*’ markers. The objective is minimized to 4.078, while the individual errors are minimized as follows:  $a_{\text{err}} = 0.170$ ,  $b_{\text{err}} = 0.197$ ,  $L_{\text{err}} = 0.4 \text{ mm}^2$ , and  $\alpha_{\text{err}} = 0.001 \text{ rad}^2$ . The time taken for optimization is 5996 seconds (about 1.67 hours).

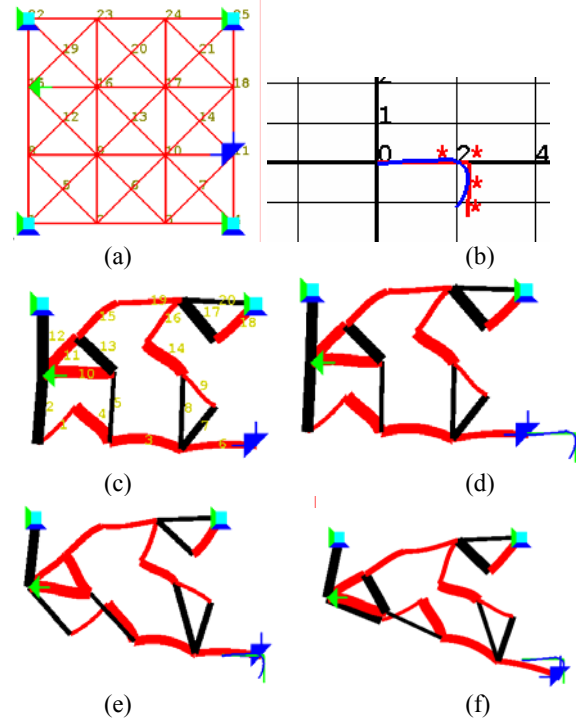
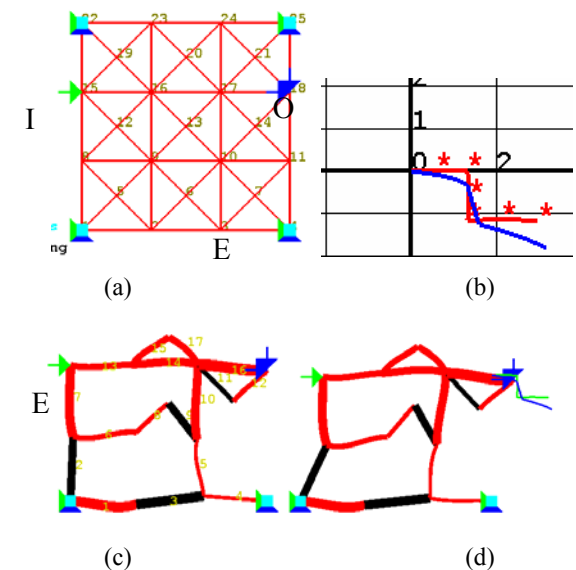


Fig. 5: Topology synthesis of a partially compliant mechanism for a prescribed ‘L’ shaped path. (a) design and input output specifications, (b) comparison between the specified path (shown as ‘\*’) and the response path (shown using solid line), (c) The optimal partially compliant mechanism. (d)-(e) Different stages of mechanism actuation illustrating how the output port traverses the path which is very close in shape, size and orientation to the prescribed ‘L’ shaped path.

### 5.2 Synthesis for a prescribed Z-shaped path



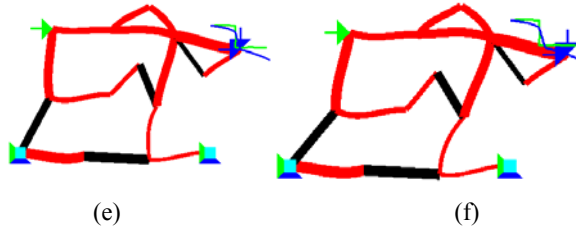


Fig 6: Synthesis of a partially compliant mechanism for a 'Z' prescribed path. (a) Design specifications, (b) comparison of response and target paths; the target path is shown using the '\*' markers, (c) the optimal mechanism, (d)-(f) different actuated positions of the mechanism showing the output port trajectory.

In this example, the base mesh is the same as that in the previous example. The arc length of the specified 'Z' shaped path is about 41 mm or approximately 41% of the characteristic dimension of the domain. No external resistance is modeled at the output port. The total number of variables is 352. Bounds for the in-plane widths are set to [2, 6] mm. Node meandering is allowed within a rectangular region of size 5×5 mm. The end slopes are optimally determined within the range of [-0.4, 0.4] rad. The upper and lower limits of the actuation force magnitude are kept the same as 30 N. The elastic modulus of the frame element is taken as 2000 Nmm<sup>2</sup> and same for the truss elements is taken as 1000 Nmm<sup>2</sup>. The coefficients for the errors in the objective are 10.0, 10.0, 1.0 and 1.0 for  $a_{err}$ ,  $b_{err}$ ,  $\alpha_{err}$  and  $L_{err}$  respectively. The number of generations for which the genetic algorithm is executed is 6000 with a population size of 40. The crossover and mutation probabilities are taken as 0.95 and 0.05 respectively. In every generation, four best individuals are copied directly to the next generation. The start point, P\* for the path is near (0.5, -2.4). The objective function for this example is minimized to 4.693. The individual errors  $a_{err}$ ,  $b_{err}$ ,  $\alpha_{err}$  and  $L_{err}$  are minimized to 0.21, 0.22, 0.17 and 0.15 respectively. The time taken for optimization is about 16295 seconds (4.53 hours). The optimized mechanism is shown in Fig 6 (c). The output paths are compared in Fig 6 (b) wherein the specified 'Z' path is shown using '\*' markers and the obtained path is depicted using a solid line. The three deformed positions of the optimal partially compliant mechanism are shown in Figs. 6 (d)-(f). As can be observed, non-smooth regions in the response path are very near to those specified in the target path.

## 6 CLOSURE

We demonstrate in this paper the topology, shape and size synthesis of partially compliant mechanisms for prescribed non-smooth paths. We employ two member types, namely the initially curved frame and truss elements that offer different local deformation and joint characteristics. The shape and size attributes of these members, i.e., the curvature, cross sections and lengths are evolved using a stochastic search. The objective formulated captures the path's shape, arc length and orientation explicitly and independently as opposed to the least squared objective based on the precision points. We present two synthesis examples, those for the prescribed 'L' shaped and 'Z'

shaped paths and observe the following: (i) the response paths obtained are very similar in shape, if not identical, to those specified and (ii) regions of non-unique or undefined slopes are captured near those specified.

## REFERENCES

- [1] Frecker, M., Ananthasuresh, G. K., Nishiwaki, N., Kikuchi, N., and Kota, S., 1997, "Topological Synthesis of Compliant Mechanisms Using Multi-criteria Optimization," *ASME J. Mech. Des.*, **119**, pp. 238–245.
- [2] Saxena, A., and Ananthasuresh, G. K., 2000, "On an Optimality Property of Compliant Topologies," *Struct. Multidiscip. Optim.*, **19**, 36–49.
- [3] Lu, K.-J., and Kota, S., 2003, "Design of Compliant Mechanisms for Morphing Structural Shapes," *J. Intell. Mater. Syst. Struct.*, **14**\_6\_, pp. 379–391.
- [4] Saxena, A., and Ananthasuresh, G. K., 2001, "Topology Synthesis of Compliant Mechanisms for Nonlinear Force-deflection and Curved Output Path," *ASME J. Mech. Des.*, **123**, pp. 33–42.
- [5] Saxena, A., 2005, "Synthesis of Compliant Mechanisms for Path Generation Using Genetic Algorithm," *ASME J. Mech. Des.*, **127**, pp. 1–8.
- [6] Saxena, A., 2005, "Topology Design of Large Displacement Compliant Mechanisms With Multiple Materials and Multiple Output Ports," *Struct. Multidiscip. Optim.*, **30**\_6\_, pp. 477–490.
- [7] Parsons, R., and Canfield, S. L., 2002, "Developing Genetic Programming Techniques for the Design of Compliant Mechanisms," *Struct. Multidiscip. Optim.*, **24**, pp. 78–86.
- [8] Zhou, H., and Ting, K. L., 2005, "Topological Synthesis of Compliant Mechanisms Using Spanning Tree Theory," *ASME J. Mech. Des.*, **127**\_4\_, pp. 753–759.
- [9] Zhou, H., and Ting, K. L., 2006, "Shape and Size Synthesis of Compliant Mechanisms Using Wide Curve Theory," *ASME J. Mech. Des.*, **128**\_3\_, pp.551–558.
- [10] Rai, A., Saxena, A., Mankame, N. D., 2007, "Synthesis of Path Generating Compliant Mechanisms Using Initially Curved Frame Elements," *ASME J. Mechanical Design*, Vol 129, pp: 1-8 to appear in October.
- [11] Mettlach, G. A., 1996, "Analysis and Design of Compliant Mechanisms Using Analytical and Graphical Techniques," Ph.D. thesis, Purdue University, West Lafayette, IN.
- [12] Mankame, N. D. and Ananthasuresh, G. K., 2007, "Synthesis of Contact-aided Compliant Mechanisms for Non-smooth Path Generation," *The International Journal for Numerical Methods in Engineering*, v. 69, pp. 2564-2605.
- [13] Ramrakhiani, D., Frecker, M., Lesieutre, G., 2006, "Hinged Beam Elements for the Topology Design of Compliant Mechanisms Using the Ground Structure Approach," *Proceedings of the ASME IDETC-06*, Paper Number 99439
- [14] Crisfield, M. A., 1991, *Nonlinear Finite Element Analysis of Solids and Structures*, John Wiley and Sons Inc., New York, Vol. 1.
- [15] Belytschko, T., and Glaum, L. W., 1979, "Applications of Higher Order Corotational Stretch Theories to Nonlinear Finite Element Analysis," *Comput. Struct.*, **10**, pp. 175–182.
- [16] Belytschko, T., and Hsieh, B. J., 1973, "Non-linear Transient Finite Element Analysis With Convected Coordinates," *Int. J. Numer. Methods Eng.*, **7**, pp. 255–271.
- [17] Mankame, N. D., 2004, "Investigations on Contact-Aided Compliant Mechanisms," Ph.D. thesis, University of Pennsylvania, Philadelphia, PA.
- [18] Ullah, I., and Kota, S., 1997, "Optimal Synthesis of Mechanisms for Path Generation Using Fourier Descriptors and Global Search Methods," *ASME J. Mech. Des.*, **119**, pp. 504–510.